Value and Limitation of Stress Thallium-201 Single Photon Emission Computed Tomography: Comparison with Nitrogen-13 Ammonia Positron Tomography

Nagara Tamaki, Yoshiharu Yonekura, Michio Senda, Keiji Yamashita, Harutoshi Koide, Hideo Saji, Tetsuo Hashimoto, Tetsuro Fudo, Hirofumi Kambara, Chuichi Kawai, and Junji Konishi

Department of Nuclear Medicine & Radiology, and The Third Division, Department of Medicine, Kyoto University School of Medicine, Kyoto, Japan

The diagnostic value of exercise ^{201}Tl single photon emission computed tomography (SPECT) for assessing coronary artery disease (CAD) was comparatively evaluated with exercise [^{13}N] ammonia positron emission tomography (PET). Fifty-one patients underwent both stress-delayed SPECT imaging using a rotational gamma camera and stress-rest PET imaging using a high resolution PET camera. Of 48 CAD patients, SPECT showed abnormal perfusion in 46 patients (96%), while PET detected perfusion abnormalities in 47 (98%). The sensitivity for detecting disease in individual coronary arteries (>50% stenosis) was also similar for SPECT (81%) and PET (88%). When their interpretations were classified as normal, transient defect, and fixed defect in 765 myocardial segments, SPECT and PET findings were concordant in 606 segments (79%). However, 66 segments showed a fixed defect by SPECT but a transient defect by PET, whereas there were only nine segments showing a transient defect by SPECT and a fixed defect by PET. PET identified transient defects in 34% of the myocardial segments showing a fixed defect by SPECT. We conclude that both stress SPECT and PET showed high and similar sensitivities for detecting CAD and individual stenosed vessels. Since stress-delayed SPECT with single tracer injection detected fewer transient defects, it may underestimate the presence of myocardial ischemia, compared with high resolution PET imaging with two tracer injections.

J Nucl Med 29:1181–1188, 1988

Thallium-201 (^{201}Tl) single photon emission computed tomography (SPECT) using a rotational gamma camera has been used for three-dimensional assessment of myocardial perfusion in coronary artery disease (CAD). It provides high diagnostic accuracy for detecting myocardial infarction (*1–3*) and stenosed vessels (*4, 5*). In addition, it is also useful for quantitative assessment of infarct size (*6*), jeopardized myocardial mass (*7*), and perfused mass (*8,9*). However, because of inherent limitations of poor resolution and relatively inadequate counts, this technique may not be suitable for assessing subtle changes in myocardial perfusion.

Myocardial perfusion study with positron emission tomography (PET) enables quantitative evaluation of tracer distribution and hence quantification of myocardial perfusion (*10–14*). We have recently reported a high diagnostic accuracy for detecting CAD of nitrogen-13 (^{13}N) ammonia and high resolution PET performed both at rest and stress (*15,16*).

Theoretically, PET provides better quality images with much higher count density and higher resolution than SPECT (*17,18*). We postulate that PET perfusion imaging may have a superior diagnostic accuracy for the evaluation of CAD compared to thallium SPECT. This study was undertaken to evaluate the clinical value and limitations of stress-redistribution thallium SPECT

Received July 27, 1987; revision accepted Dec. 30, 1987.

For reprints contact: Nagara Tamaki, MD, Dept. of Nuclear Medicine & Radiology, Kyoto University School of Medicine, Shogoin, Sakyo-ku, Kyoto, 606, Japan.

in the study of coronary artery disease in comparison with stress-rest [^{13}N]ammonia PET.

MATERIALS AND METHODS

Patient Population

Fifty-one patients who were referred for coronary angiography underwent both stress thallium SPECT and stress [^{13}N] ammonia PET. The age ranged from 34 to 71 yr with a mean value of 56.1 yr old. Thirty-eight patients had a history of myocardial infarction. The mean interval from the most recent infarction to the study was 17 mo (range 1 to 96 mo).

Coronary angiography was performed in multiple views. Three experienced observers reviewed the coronary angiograms without knowledge of the radionuclide data. The narrowing was graded according to the lumen diameter involved: 25% or less, 26 to 50%, 51 to 75%, 76 to 90%, 91 to 99% or 100% (*5*). The consensus was used in the data analysis. All but three patients had significant stenosis (>50% in diameter) in at least one of the major coronary arteries. Eighteen had single-vessel disease, 17 had two-vessel disease, and 13 had three-vessel disease.

All patients gave informed consent.

Stress Thallium SPECT Imaging

Exercise was performed using an upright bicycle ergometer. The exercise level started at 25 W and increased an additional 25 W every 3 min. Each patient exercised to 85% of the age predicted maximal heart rate, the onset of angina pain, dyspnea, ST segment depression (0.2mV) or to a decrease in blood pressure. One minute before completion of exercise, 2.5–3 mCi (93 to 111 MBq) of thallium-201 (^{201}Tl) chloride was injected intravenously.

Tomographic acquisition started ~5 min (stress stage) and 3 hr (delayed stage) after thallium injection using a rotating gamma camera (General Electric 400 ACT) with a low-energy, general purpose collimator interfaced to a digital computer (General Electric MaxiStar). The camera was rotated at 5.6-degree increments of revolution from 45-degree left posterior oblique to 45-degree right anterior oblique position of the patient, collecting 32 views over 180-degree for 30 sec each (*4,5*). System resolution in reconstructed images was 17 mm at full width half maximum (*4,5*).

A series of contiguous transverse slices of the left ventricular myocardium were reconstructed by filtered back projection with Ramp-Hanning filter with a cutoff frequency of 0.5 cycle/pixel. Attenuation correction was not performed. These images were further processed to obtain the short-axis and long-axis sections perpendicular to the cardiac axes. Multiple sections with 6–12 mm thickness were obtained in each tomographic plane. Each reconstructed slice contained 15,000 to 28,000 counts.

Stress [^{13}N]Ammonia PET Imaging

Nitrogen-13 ammonia was produced by ^{16}O(p,α)^{13}N nuclear reaction with water irradiation using an ultracompact cyclotron (Sumitomo Heavy Industry, CYPRIS 325), followed by a reduction to [^{13}N]ammonia with titanous hydroxide. The [^{13}N]ammonia was collected in a saline solution and passed through a Millipore filter (*16*).

PET study was performed within 2 wk of the thallium SPECT study using a whole-body multislice PET camera (Hitachi, Positologica III) which provided seven tomographic slices at 16 mm intervals simultaneously (*19*). The spatial resolution was 7.6 mm and the axial resolution was 12.6 mm at full width half maximum at the center of field (*19*).

First, the patient was positioned in the gantry to obtain transmission images using a rotating ^{68}Ge/^{68}Ga standard plate source for attenuation correction through the body. While the patient lay on the bed at rest, 10–15 mCi (370 to 555 MBq) of [^{13}N]ammonia was injected intravenously as a bolus. Three minutes later, myocardial PET scanning was performed for 5 min. Immediately following the first PET scanning, the second PET scanning was carried out for 8 min to obtain interpolating PET images. These two PET scannings provided a total of 14 contiguous slices of the myocardium with 8-mm intervals (*20*).

Two hours after the initial study, a stress PET study was performed. The exercise was carried out using a supine bicycle ergometer attached to a PET patient bed. The exercise protocol was the same as for the stress thallium study. Another dose of [^{13}N]ammonia (370–555 MBq) was injected at peak exercise level and the exercise was continued for another 30 sec after the injection. The patient was carefully positioned in the PET gantry according to the orientation lines marked at the initial study. Stress myocardial PET imaging was performed 3 min after the injection for 5 min, followed by the interpolating PET scanning as described in the resting study. Each PET image contained ~2 to 3 million counts.

Analysis of the Images

The SPECT and PET images were independently interpreted by three experienced observers without knowledge of coronary angiographic data. In addition, three transverse slices, upper, middle and lower sections of the myocardium were selected from the SPECT and PET images for circumferential profile analysis (*21*). To ensure that the same segments in the same slice was compared on stress and resting (delayed) images, a series of transverse slices were displayed before the selection of the three slices of stress and resting perfusion images. The left ventricular myocardium was divided into 60 radial segments at 6-degree intervals from the center of the left ventricular cavity. Each circumferential profile curve was compared to those of 12 normal subjects for objective assessment of perfusion abnormalities (*6,16*). The areas with perfusion below the lower limits covering at least 30 degrees of the circumferential profiles were considered as perfusion defects. To detect the presence of transient perfusion defects, the resting and stress profile curves of the same slice were compared. When the % change in perfusion was >10% at stress compared to the resting perfusion, the areas were defined as transient perfusion defects.

From the segmental analysis of stress images for visual and objective assessment, the left ventricular myocardium was divided into 15 myocardial segments from the three transverse slices (Fig. 1). A perfusion abnormality in the inferior and posterior walls was defined as a right coronary artery (RCA) (or posterior descending artery) lesion, that in the septal and anterior walls as a left anterior descending artery (LAD) lesion and that in the posterolateral wall as a left circumflex (LCX) lesion (*4–6,15,16*) (Fig. 1). In patients with left circumflex dominant or balanced coronary artery distribution, the posterior descending artery was considered to belong to the right coronary artery. When the equivocal hypoperfusion in inferior

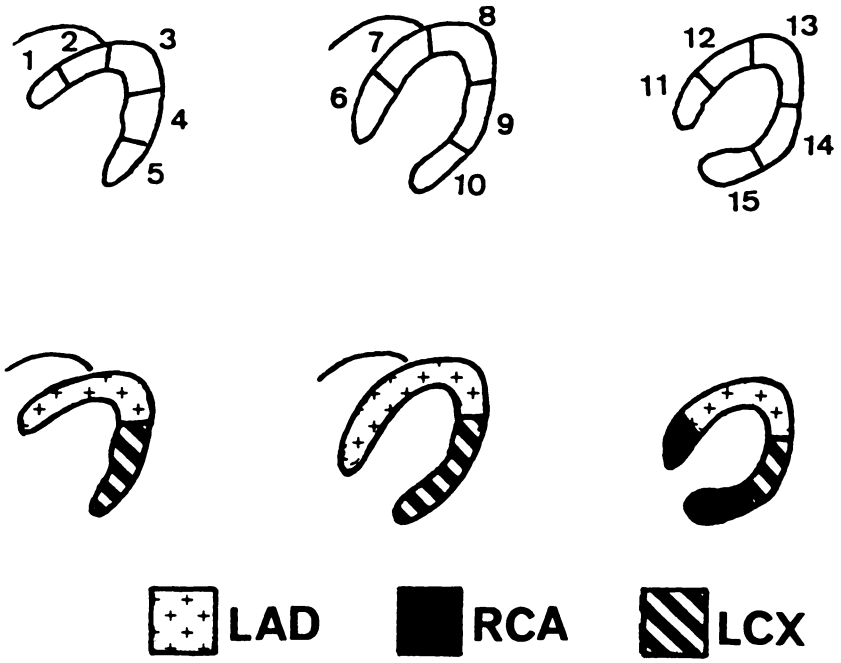

FIGURE 1
Schematic presentation of three transverse slices obtained from SPECT and PET studies showing 15 myocardial segments, and the distribution of three major coronary arteries: left anterior descending artery (LAD), right coronary artery (RCA), and left circumflex artery (LCX).

and posterior segments was present, the short-axis and long-axis sections were used for assessing RCA lesions (*1,5,20*).

The observers assessed both images and profile curves to determine the presence of abnormalities, their location and the presence of transient perfusion abnormalities. The consensus was used in the data analysis.

Statistical Analysis

Sensitivity was defined as the number of true-positive tests divided by the sum of true-positive and false-negative tests. Specificity was defined as the number of true-negative tests divided by the sum of true-negative and false-positive tests. The chi-square test with or without Yate's correction was used to determine the significance of a difference in observed rates of occurrence. The difference in exercise levels was determined with two-tailed Student's t-test. A significant difference was considered to exist when a probability (p) value of 0.05 or less was observed.

RESULTS

Exercise Levels

The peak heart rate obtained during the SPECT study was higher (130 ± 16) (mean ± s.d.) than the PET study (121 ± 15) ($p < 0.001$). The pressure rate product was also higher in the former (20,900 ± 4,900 versus 19,100 ± 4,400) ($p < 0.001$). This difference is considered to be due to the upright ergometer exercise during the SPECT study compared to the supine exercise during the PET study.

Diagnosing Coronary Artery Disease

Of 48 patients with angiographically documented coronary artery disease, stress thallium SPECT showed abnormal perfusion in 46 (96%), while stress [^{13}N] ammonia PET showed abnormal perfusion in 47 (98%). Three angiographically normal subjects did not reveal any perfusion abnormalities by either SPECT or PET.

Detecting Individual Vessel Involvement

Segmental perfusion analysis was performed by stress SPECT and PET for detecting disease in individual coronary arteries (Tables 1 and 2). In 91 stenosed vessels, the sensitivity was similar for stress thallium SPECT (81%) and [^{13}N]ammonia PET (88%). The values were similar for detecting RCA lesion (79% vs 76%), LAD lesion (90% versus 93%) and LCX lesion (65% versus 85%), respectively (Table 1). When the

TABLE 1
Sensitivity for Detecting Disease in Individual Coronary Arteries by Stress Thallium SPECT and [^{13}N]ammonia PET

	Overall			Infarct Segments			Noninfarct Segments		
	SPECT	PET	(Sig)*	SPECT	PET	(Sig)	SPECT	PET	(Sig)
RCA	23/29 (79%)	22/29 (76%)	(N.S.)†	14/17 (82%)	14/17 (82%)	(N.S.)	9/12 (75%)	8/12 (67%)	(N.S.)
LAD	38/42 (90%)	39/42 (93%)	(N.S.)	22/23 (96%)	23/23 (100%)	(N.S.)	16/19 (84%)	16/19 (84%)	(N.S.)
LCX	13/20 (65%)	17/20 (85%)	(N.S.)	6/6 (100%)	6/6 (100%)	(N.S.)	7/14 (50%)	11/14 (79%)	(N.S.)
Overall	74/91 (81%)	80/91 (88%)	(N.S.)	42/46 (91%)	43/46 (93%)	(N.S.)	32/45 (71%)	35/45 (78%)	(N.S.)

* Significance.
† Not significant.

individual vessels were subdivided into those supplying infarcted and noninfarcted segments, similar sensitivities were observed by SPECT and PET for the detection of stenosed vessels supplying noninfarcted segments (71% versus 78%) as well as infarcted segments (91% versus 93%), respectively (Table 1).

The specificity for the detection of the absence of disease in individual vessels is listed in Table 2. The overall specificity was 92% by thallium SPECT and 89% by PET. Among the vessels which revealed abnormal perfusion by SPECT and PET, two had insignificant (25–50%) stenosis by coronary angiography. The specificity was similar for detecting absence of RCA lesions (95% versus 86%), LAD lesions (89% versus 100%) and LCX lesions (93% versus 90%), respectively.

Thus, the diagnostic values for detecting the presence or absence of disease in individual vessels were similar for SPECT and PET.

Interpretation of Perfusion

The correlations of interpretation for each myocardial segment by stress SPECT and PET studies are summarized in Table 3. Of 765 total myocardial segments, both SPECT and PET were normal in 393 segments (51%), showed a transient perfusion defect in 107 segments (14%) and showed a fixed perfusion defect in 106 segments (14%). Thus, their interpretation was matched in 606 segments (77%).

There were 66 segments (9%) showing a transient defect by PET but a fixed defect by SPECT. On the other hand, only nine segments (1%) showed a fixed defect by PET and transient defect by SPECT ($p < 0.001$). Consequently, PET identified transient defects in 34% of the myocardial segments showing a fixed defect by SPECT.

Figure 2 shows two representative slices of stress and resting perfusion images obtained by SPECT and PET in a patient with two-vessel disease. Both images showed a transient perfusion defect in the anteroseptal wall. They also showed slight hypoperfusion in inferior wall at both rest and stress, which was better visualized by short-axis sections by SPECT.

Figure 3 shows stress and resting perfusion images obtained by SPECT and PET in a patient with three-vessel disease. Thallium SPECT images showed similar hypoperfusion in anteroseptal, apical and posterolateral areas at both rest and stress. On the other hand, [^{13}N]ammonia PET images showed an additional decrease in perfusion in apical through posterolateral areas at stress compared to mild hypoperfusion in the same area at rest. Figure 4 shows the circumferential profile curves of stress and resting perfusion of the representative SPECT and PET slices. Perfusion in the apical through posterolateral segments was similarly decreased at rest and stress by SPECT, while the stress induced hypoperfusion was clearly demonstrated in the same area by PET. Stress induced hypoperfusion in this area by PET suggests the presence of myocardial ischemia, which was not suggested by SPECT.

TABLE 2
Specificity for Detecting Absence of Disease in Individual Coronary Arteries by Stress SPECT and PET

	SPECT	PET	Significance
RCA	21/22 (95%)	19/22 (86%)	N.S.
LAD	8/9 (89%)	9/9 (100%)	N.S.
LCX	29/31 (94%)	29/31 (94%)	N.S.
Overall	58/62 (94%)	56/62 (90%)	N.S.

TABLE 3
Correlation of Interpretations of Myocardial Segments by Stress Thallium SPECT and [^{13}N]Ammonia PET

		SPECT			
		Normal	Transient defect	Fixed defect	Overall
PET	Normal	393	18	25	436
	Transient defect	22	107	66	195
	Fixed defect	19	9	106	134
	Overall	434	134	197	765

DISCUSSION

This comparative study demonstrated that stress thallium SPECT study provides as high a sensitivity for detecting coronary artery disease and identifying disease in individual coronary arteries as does stress [^{13}N]ammonia PET imaging.

Both tomographic techniques have the advantages for three-dimensional assessment of myocardial perfusion compared to the planar imaging. They permit better visualization of segmental perfusion, particularly in deep myocardial regions which may allow detection of regions with lesser ischemia as hypoperfused areas (*5,22*). The sensitivity reported in the present study is similar to our previous studies (*4,5,15,16*) and to other studies (*7,23,24*).

Although the exercise level in the PET study was lower than that in the SPECT study, stress PET imaging provided a similar sensitivity. In this sense, this high resolution tomographic imaging may further enhance the detection of a region of lesser myocardial ischemia. To verify this hypothesis, another comparative study for detecting milder coronary lesions between SPECT and PET using the same exercise load may be warranted.

On the other hand, stress SPECT which also provides reorientation of the data into cardiac short-axis and long-axis sections of the heart enables a superior three-dimensional assessment of myocardial perfusion. The-

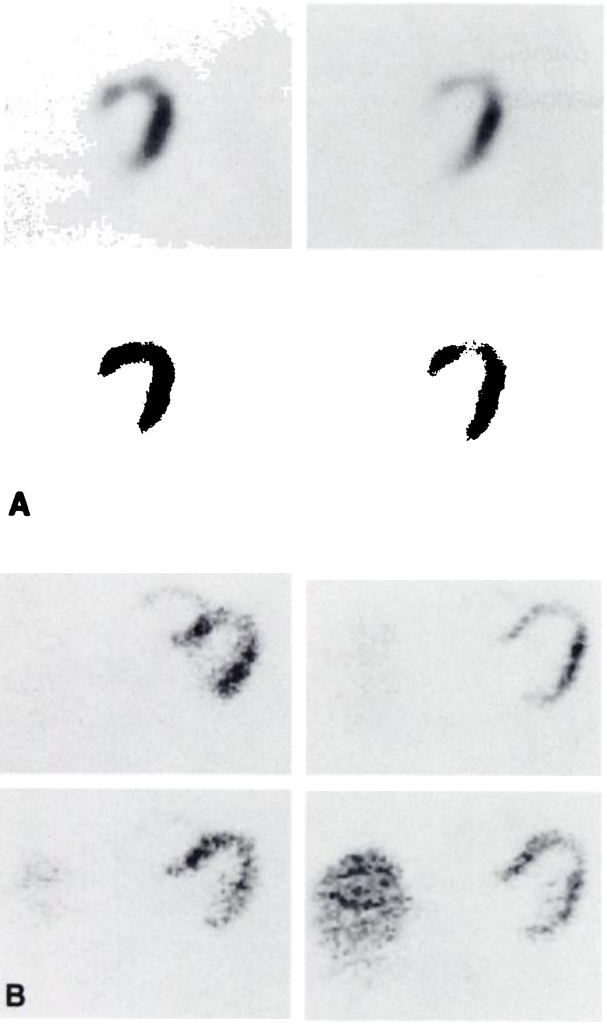

FIGURE 2
Two representative slices of stress-delayed thallium SPECT images (A) and stress-rest [^{13}N]ammonia PET images (B) of a patient with two-vessel disease. Both studies demonstrated transient perfusion defect in anteroseptal wall.

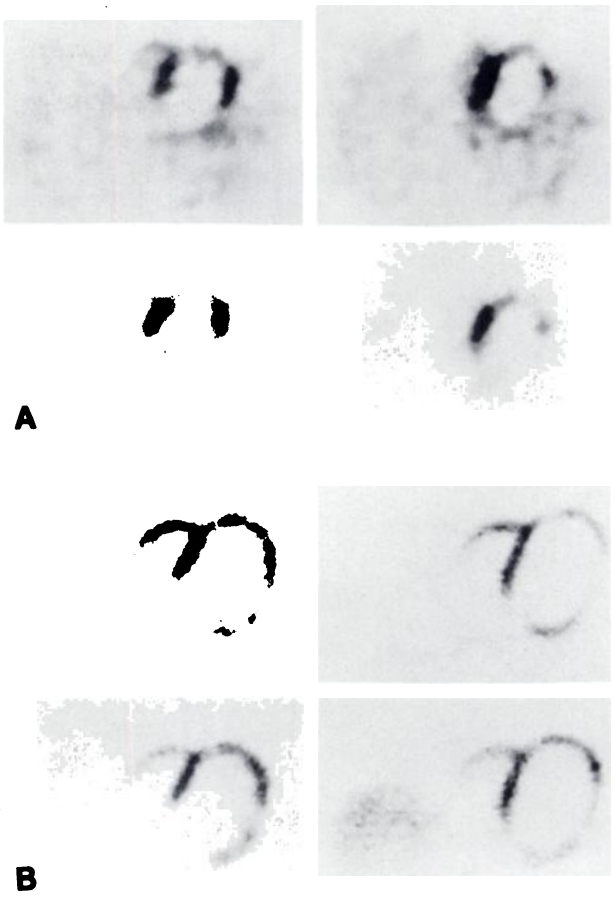

FIGURE 3
Two representative slices of stress-delayed thallium SPECT images (A) and stress-rest [^{13}N]ammonia PET images (B) of a patient with three-vessel disease. SPECT study shows fixed perfusion defect in anterior, apical and posterolateral regions, whereas PET demonstrated transient defect in the same area.

oretically SPECT might be superior for evaluating lesions in inferior regions compared to PET imaging, which provides only transverse sections of the heart (*18*). However, this comparative study did not show a statistically significant difference in the diagnostic values for detecting right coronary lesions. Furthermore, recent advances in computer software enable reconstruction of oblique-angle tomograms perpendicular to the cardiac axes in PET as well (*20*).

It is of clinical importance to differentiate ischemic and viable myocardial regions from irreversible and infarcted regions. Analysis of thallium redistribution has been considered to be useful for detection of ischemic but viable myocardium (*25*). Reduced initial thallium uptake that redistributes in delayed images (transient perfusion detect) usually represents viable myocardium, whereas an initial thallium defect that persists with time is considered to represent nonviable infarcted myocardium. However, in some regions with a fixed perfusion defect on a preoperative study, significant improvements in perfusion and cardiac function have been observed after coronary revascularization (*26*) or coronary angioplasty (*27*). In addition, recent preliminary PET data by us (*28*) and by Brunken et al. (*29*) described metabolically active areas in some fixed perfusion defects by thallium imaging. These data suggest that fixed perfusion defects on thallium scan do not necessarily mean irreversible infarcted myocardium. The present study also demonstrated that high resolution PET with two separate injections of the tracer can depict transient perfusion defects in approximately one-third of the segments showing a fixed defect by stress-delayed thallium SPECT with single injection. Thus, analysis of redistribution by stress thallium scan, even with three-dimensional tomographic technique, may underestimate the presence of myocardial ischemia.

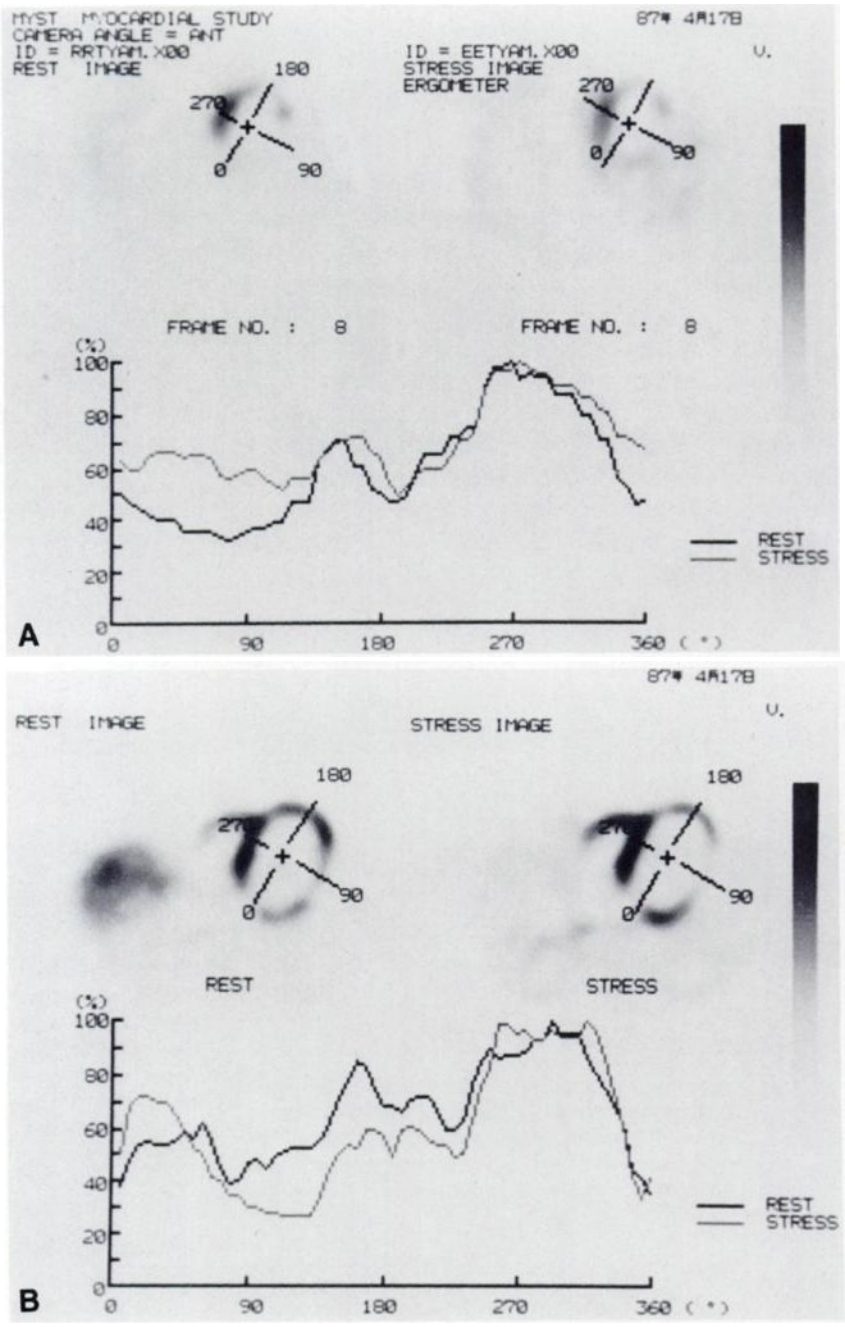

FIGURE 4
The circumferential profile curves of stress-delayed SPECT images (A) and stress-rest PET images of one representative slice in the same patient as Figure 3. These curves also demonstrated similar perfusion abnormalities both stress and rest by SPECT, whereas stress induced hypoperfusion by PET.

Several mechanisms may be considered for this phenomenon. In these segments, the coronary flow was quite reduced, so that no redistribution was observed or redistribution occurred too slow to be seen within 3 hr. In addition, when the blood concentration of thallium was low during postexercise period, the lack of redistribution may often be observed in noninfarcted myocardial segments (*30*). Therefore, stress induced hypoperfusion can only be delineated by two separate injection of the tracer at rest and during exercise, such as with PET imaging. In this respect, the preliminary reports describing the value of a 24-hr delayed scan for detecting redistribution which was not observed at 3 hr (*31–33*) seem to be attractive. However, because of inadequate count density of thallium, the image quality of thallium SPECT at 24 hr after injection may often be too degraded to assess substantial changes in tracer distribution.

Another potential reason for the detection of more transient defects by PET is the higher resolution and higher count density images of PET (*17,18*). Consequently, it can delineate even subtle changes in tracer distribution at stress as compared to resting distribution.

A difference in tracer kinetics between thallium and [^{13}N]ammonia may also be considered. Particularly metabolic changes of [^{13}N]ammonia after trapping in

the myocardium may potentially explain this difference (*34*). In this respect, transient perfusion defects by PET may not represent myocardial ischemia. However, our preliminary data showed a frequent FDG uptake in the regions with transient [^{13}N]ammonia perfusion defects, indicating the presence of metabolic activity in these areas (*35*). Furthermore, since a good correlation was observed between [^{13}N]ammonia uptake and myocardial blood flow measured by microspheres, particularly in low flow range (*11*), a significant difference in tracer kinetics in an ischemic region may be less likely.

Although PET provides high quality images of myocardial perfusion, it is not widely available at present. A generator system combined with PET may enhance the clinical feasibility of PET study for assessing myocardial perfusion in the near future (*36*).

We conclude that thallium SPECT and [^{13}N]ammonia PET provide high and similar sensitivities for detecting coronary artery disease and individual stenosed vessels. But stress-delayed SPECT with single tracer injection detects transient perfusion defects less commonly than stress-rest PET with two separate injections, which indicates that the current thallium SPECT study may underestimate the presence of myocardial ischemia.

ACKNOWLEDGMENTS

The authors acknowledge the technical assistance of Takao Mukai, Yutaka Konishi, Masataka Hayashi, Eriko Komori, and Toru Fujita. This work was supported in part by Japanese Ministry of Education Grant #62770782.

REFERENCES

1. Tamaki N, Mukai T, Ishii Y, et al. Clinical evaluation of thallium-201 single-photon transaxial tomography using a rotating gamma camera: comparison with seven-pinhole tomography. *J Nucl Med* 1981; 22:849–855.
2. Maublant J, Cassagnes J, LeJeune JJ, et al. A comparison between conventional scintigraphy and emission tomography with thallium-201 in the detection of myocardial infarction. *J Nucl Med* 1982; 23:204–208.
3. Ritchie JL, Williams DL, Harp G, et al. Transaxial tomography with thallium-201 for detecting remote myocardial infarction. *Am J Cardiol* 1982; 50:1236–1241.
4. Nohara R, Kambara H, Suzuki Y, et al. Stress scintigraphy using single-photon emission computed tomography (SPECT) in the evaluation of ischemic heart disease. *Am J Cardiol* 1984; 53:1250–1254.
5. Tamaki N, Yonekura Y, Mukai T, et al. Stress thallium-201 transaxial emission computed tomography: quantitative versus qualitative analysis for evaluation of coronary artery disease. *J Am Coll Cardiol* 1984; 4:1213–1221.
6. Tamaki S, Nakajima H, Murakami T, et al. Estimation of infarct size by myocardial emission computed tomography with thallium-201 and its relation to creatine kinase-MB release after myocardial infarction in man. *Circulation* 1982; 66:994–1001.
7. Pringent F, Maddahi J, Garcia E, et al. Noninvasive quantification of the extent of jeopardized myocardium in patients with single-vessel coronary disease by stress thallium-201 single-photon emission computerized tomography. *Am Heart J* 1986; 111:578–586.
8. Holman BL, Moore SC, Shulkin PM, et al. Quantitation of perfused myocardial mass using Tl-201 and emission computed tomography. *Invest Radiol* 1983; 18:322–326.
9. Wolfe CL, Lewis SE, Corbett JR, et al. Measurement of myocardial infarction fraction using single photon emission computed tomography. *J Am Coll Cardiol* 1985; 6:145–151.
10. Schelbert HR, Phelps ME, Hoffman EJ, et al. Regional myocardial perfusion assessed with N-13 labeled ammonia and positron emission computerized axial tomography. *Am J Cardiol* 1979; 43:209–218.
11. Schelbert HR, Phelps ME, Huang SC, et al. N-13 ammonia as an indicator of myocardial blood flow: factors influencing its uptake and retention in myocardium. *Circulation* 1981; 63:1259–1272.
12. Wisenberg G, Selin CE, Child J, Skorton D, et al. In vivo quantitation of regional myocardial blood flow by positron-emission computed tomography. *Circulation* 1981; 63:1248–1258.
13. Mullani NA, Goldstein RA, Gould KL, et al. Myocardial perfusion with rubidium-82: I. Measurement of extraction fraction and flow with external detector. *J Nucl Med* 1983; 24:898–906.
14. Bergmann SR, Fox KA, Rand AL, et al. Quantification of regional myocardial blood flow in vivo with $H_2{}^{15}O$. *Circulation* 1984; 70:724–733.
15. Tamaki N, Yonekura Y, Senda M, et al. Myocardial positron computed tomography with ^{13}N-ammonia at rest and during exercise. *Eur J Nucl Med* 1985; 11:246–251.
16. Yonekura Y, Tamaki N, Senda M, et al. Detection of coronary artery disease with ^{13}N-ammonia and high resolution positron-emission computed tomography. *Am Heart J* 1987; 113:645–654.
17. Budinger TF, Derenzo SE, Gullberg GT, et al. Emission computer assisted tomography with single-photon and positron annihilation photon. *J Comput Assist Tomogr* 1977; 1:131–145.
18. Tamaki N, Yonekura Y, Senda M, et al. Comparative study of myocardial perfusion imaging by Tl-201 single-photon ECT and N-13 ammonia positron CT [Abstract]. *J Nucl Med* 1984; 25:P6.
19. Senda M, Tamaki N, Yonekura Y, et al. Performance characteristics of Positologica III, a whole body positron emission tomograph. *J Comput Assist Tomogr* 1985; 9:940–946.
20. Senda M, Yonekura Y, Tamaki N, et al. Interpolating scan and oblique-angle tomograms in myocardial PET using nitrogen-13 ammonia. *J Nucl Med* 1986; 27:1836–1980.
21. Burow RD, Pond M, Schafer AW, et al. "Circumferential profiles" a new method for computer analysis of thallium-201 myocardial perfusion images. *J Nucl Med* 1979; 20:771–777.
22. Gould KL, Schelbert HR, Phelps ME, et al. Noninvasive assessment of coronary stenosis with myocardial perfusion imaging during pharmacologic coronary vasodilation. V. Detection of 47 percent diameter

coronary stenosis with intravenous nitrogen-13 ammonia and emission-computed tomography in intact dogs. *Am J Cardiol* 1979; 43:200–208.
23. Garcia EV, Train KV, Maddahi J, et al. Quantification of rotational thallium-201 myocardial tomography. *J Nucl Med* 1985; 26:17–26.
24. Garcia E, DePuey EG, Brown M, et al. Quantification of rotational thallium-201 myocardial tomograms: a multicenter trial using bullseye polar maps and standard normal limits [Abstract]. *J Nucl Med* 1987; 28:673.
25. Pohost GM, Zir LM, Moore RH, et al. Differentiation of transiently ischemic from infarcted myocardium by serial imaging after a single dose of thallium-201. *Circulation* 1977; 55:294–302.
26. Gibson RS, Watson DD, Taylor GJ, et al. Prospective assessment of regional myocardial perfusion before and after coronary revascularization surgery by quantitative thallium-201 scintigraphy. *J Am Coll Cardiol* 1983; 3:804–815.
27. Liu P, Kiess MC, Okada RD, et al. The persistent defect on exercise thallium imaging and its fate after myocardial revascularization: Does it represent scar or ischemia? *Am Heart J* 1985; 110:996–1001.
28. Tamaki N, Yonekura Y, Senda M, et al. Value and limitation of stress Tl-201 tomography. Comparison with perfusion and metabolic imaging with positron tomography [Abstract]. *Circulation* 1987; 76:IV–4.
29. Brunken R, Schwaiger M, Grover-McKay M, et al. Positron emission tomography detects tissue metabolic activity in myocardial segments with persistent thallium perfusion defects. *J Am Coll Cardiol* 1987; 10:557–567.
30. Budinger TH, Pohost GM, Bischoff P. Thallium-201 integral blood concentration over 2 hours explains persistent defects in patients with no evidence of MI by ECG [Abstract]. *Circulation* 1987; 76:IV–64.
31. Weiner SN, Flynn MJ, Edelstein J. Thallium-201 myocardial redistribution imaging 24 hours following stress exercise. *Radiology* 1981; 138:667–669.
32. Muto T, Okabe A, Okuzumi I, et al. Assessment of thallium-201 late redistribution in exercise myocardial SPECT [Abstract]. *J Nucl Med* 1986; 27:900.
33. Kiat H, Maddahi J, Yang LD, et al. Late reversibility of thallium-201 (Tl-201) myocardial tomographic defects: an accurate marker of myocardial viability [Abstract]. *Circulation* 1987; 76:IV–64.
34. Bergmann SR, Hack S, Tewson T, et al. The dependence of accumulation of $^{13}NH_3$ by myocardium on metabolic factors and its implications for quantitative assessment of perfusion. *Circulation* 1981; 61:34.
35. Yonekura Y, Senda M, Saji H, et al. Increased accumulation of fluorodeoxyglucose in stress induced myocardial ischemia [Abstract]. *J Nucl Med* 1986; 27:933.
36. Gould KL, Goldstein RA, Mullani NA, et al. Noninvasive assessment of coronary stenosis by myocardial perfusion imaging during pharmacologic coronary vasodilation. VII. Clinical feasibility of positron cardiac imaging without a cyclotron using generator-produced rubidium-82, *J Am Coll Cardiol* 1986; 7:775–789.